Structural and Valence Changes of Europium Hydride Induced by Application of High-Pressure H_2

T. Matsuoka,[1,*] H. Fujihisa,[2] N. Hirao,[1] Y. Ohishi,[1] T. Mitsui,[3,4] R. Masuda,[3] M. Seto,[5,3,4] Y. Yoda,[1,4] K. Shimizu,[6] A. Machida,[3] and K. Aoki[3]

[1]Japan Synchrotron Radiation Research Institute (JASRI)/SPring-8, Hyogo 679-5198, Japan
[2]RIIF, National Institute of Advanced Industrial Science and Technology (AIST), Ibaraki 305-8565, Japan
[3]Quantum Beam Science Directorate, Japan Atomic Energy Agency, Hyogo 679-5148, Japan
[4]CREST, Japan Science and Technology Agency, Saitama 332-0012, Japan
[5]Research Reactor Institute, Kyoto University, Osaka 590-0494, Japan
[6]KYOKUGEN, Center for Quantum Science and Technology under Extreme Conditions, Osaka University, Osaka 560-8531, Japan
(Received 6 April 2011; published 5 July 2011)

Europium hydride EuH_x, when exposed to high-pressure H_2, has been found to exhibit the following structural and valence changes: $Pnma(x = 2, \text{divalent}) \rightarrow P6_3/mmc(x = 2, 7.2\text{–}8.7\ \text{GPa}) \rightarrow I4/m(x > 2, 8.7\text{–}9.7\ \text{GPa}) \rightarrow I4/mmm(x > 2, 9.7\ \text{GPa}-, \text{trivalent})$. With a trivalent character and a distorted cubic fcc structure, the $I4/mmm$ structure is the β phase commonly observed for other rare-earth metal hydrides. Our study clearly demonstrates that EuH_x is no longer an irregular member of the rare-earth metal hydrides.

DOI: 10.1103/PhysRevLett.107.025501 PACS numbers: 61.05.cp, 61.66.Fn, 76.80.+y

The ability of rare-earth metals R (where rare-earth metals, R, include yttrium (Y) and scandium (Sc)) to absorb large amounts of hydrogen (e.g., 300 mol% in YH_3, at ambient pressure) has led to extensive studies of their physical and chemical properties for the purpose of industrial applications and academic interest.

Systematic studies of RH_x have revealed common features in the crystal structure. RH_x crystallizes into essentially three structural phases, α, β and γ, depending on the hydrogen composition of $x = H/R$. The α phase is a solid solution where H atoms are distributed statistically at tetrahedral (T) interstitial sites of the metal lattice as impurities. The β phase has fcc structure. In dihydrides, H-atoms occupy T sites, forming fcc fluorite structure. The β phase has been observed for dihydrides, with ideal composition RH_2, and several trihydrides RH_3 (for $R =$ La, Ce, or Pr) [1]. Frequently noted stoichiometric defects, $RH_{2\text{-}\delta}$, are caused by impurities and structural defects. The γ phase has an hcp structure with ideal composition RH_3 ($R = Y$, Nd, Sm, Gd, Tb, Dy, Ho, Er, or Lu) [1]. It is known to transform to an fcc structure at high pressures [2–5].

Europium hydride EuH_x has been considered as an irregular member among the RH_x family, because of its unique structural properties. Reflecting its divalent ground state $4f^{n+1}(5d6s)^2$, the dihydride EuH_2 crystallizes into orthorhombic $Pnma$ ($PbCl_2$-type, Z(Eu) = 2) structure. EuH_x is the only rare-earth metal hydride for which other structural phases, including the β phase, have not been reported. Even in a high-temperature H_2 atmosphere, x does not exceed 2. Only one possible structural transition into a cubic phase has been reported under a pressure of 8 GPa [6]. This is in contrast to divalent rare-earth metal ytterbium. YbH_2 shares the $Pnma$ structure with EuH_2 at ambient pressure. When x exceeds 2.2 in YbH_x, the cubic β and β'' phases, in which only lattice parameters differ, appear. The β and β' phases, in Yb^{2+} and Yb^{3+}, are mixed valent and trivalent states, respectively [7–9].

When EuH_2 is compressed under high-pressure H_2, one can expect an increase in the hydrogen composition and valence changes that lead to structural phase transitions. The chemical potential of hydrogen on hydrogen solubility is significantly enhanced by high pressures exceeding 1 GPa [10]. The valence state of Eu can be changed between $4f^{n+1}(5d6s)^2$ and $4f^n(5d6s)^3$ by high pressure or by chemical manipulation. Thus, at a sufficiently high pressure, the β or γ phase may result from additional hydrogen uptake and a valence transition.

The aim of this study is to establish a clear connection between the structural phases of EuH_x with the other rare-earth metal hydrides, and to contribute to a fuller understanding of the interaction between hydrogen and rare-earth metals. In particular, we are interested in phase transformations and valence states of EuH_x under H_2 pressures that exceed 1 GPa to identify known phases of other "regular" RH_x.

We performed x-ray diffraction (XRD) and synchrotron Mössbauer spectroscopy measurements of two europium hydrides compressed in H_2 and He enviroments, respectively. These systems are denoted as EuH_x/H_2 and EuH_2/He, respectively. EuH_x compressed in H_2 above 9 GPa was found to yield a β phase with a tetragonal $I4/mmm$ structure in which the hydrogen composition x exceeded 2 and the valence transition $Eu^{2+} \rightarrow Eu^{3+}$ occurred. The $I4/mmm$ structure is a slightly (0.8%) distoreted fcc structure, with a c/a ratio of 1.425, and is categorized in the β phase, commonly observed in other rare-earth metal hydrides. EuH_x is thus no longer an irregular member of the rare-earth metal hydrides, as it shares their common structure.

In the experiments on the EuH_x/H_2, a high-purity Eu metal sample (99.98% metals basis, obtained from the Materials Preparation Centre of the Ames Laboratory) and fluid H_2 were packed in the sample chamber of a diamond anvil cell. Successful synthesis of EuH_2 was confirmed by observing the *Pnma* structure by XRD at the lowest pressure of 2.7 GPa. In the experiment of the EuH_2/He, an EuH_2 powder sample (99.9%, purchased from Kojundo Chmical Laboratory Co., Ltd.) was loaded into a sample chamber with fluid He. A cryogenic gas loading method was employed for the loading fluid H_2 and He. The pressure was determined from ruby-R_1 fluorescence line using the pressure scale by Mao *et al*, [11]. High-pressure XRD experiments were performed at BL10XU in SPring-8 using monochromatic synchrotron radiation and an imaging plate detector at room temperature [12]. The x-ray beam of wavelength $\lambda = 0.41299$ Å was focused with a polymer compound refractive lens (SU-8 produced by ANKA). Two-dimensional (2D) Debye-Scherrer rings were obtained and converted to 1D 2θ-intensity profiles with the software PIP [13]. Energy-domain Mössbauer spectroscopy measurements were performed on EuH_x/H_2 at pressures of up to 14 GPa at BL09XU in SPring-8, using the well-known trivalent material EuF_3 as a reference [14].

The crystal structures under high pressures were investigated by XRD measurements. Figure 1 shows typical XRD profiles in each pressurized system of EuH_x/H_2 and EuH_2/He. Weak diffraction peaks originating from oxidized EuO were observed but these are easily distinguishable from EuH_x peaks. In both EuH_x/H_2 and EuH_2/He, the *Pnma* structure was stable up to 7.2 GPa. At 7.2 GPa, the *Pnma* structure transformed to a hexagonal structure and subsequently to a tetragonal structure at 8.7 GPa. The inset graph of Fig. 1 is a magnification of the XRD profile for this tetragonal phase, obtained when the pressure was released to 4.3 GPa. The downward arrows indicate the satellite peaks for this tetragonal structure. Above 9 GPa, the satellite peaks disappeared and the split main-peaks overlapped. The XRD profile at 9.7 GPa shows the variability of the peak widths. As demonstrated in the analysis below, the sample has a tetragonal structure above 9 GPa. We provisionally name these *Pnma*, hexagonal, lower-pressure tetragonal and higher-pressure tetragonal phases as EuH_x -I, EuH_x -II, EuH_x -III, and EuH_x-IV, respectively, to indicate their order of formation. EuH_x-II is stable up to 28 GPa in EuH_2/He system. Here, it is clear that the transition I → II is a thermodynamic effect by external pressure and that II → III → IV transformations are induced by the reaction between the sample and surrounding high-pressure H_2. We note that the previously reported high-pressure phases of pure-Eu [15–17] were not observed in measurements performed on both EuH_x/H_2 and EuH_2/He systems. In addition, no abrupt decrease in diffraction intensities was observed, which suggests that EuH_x does not decompose in the range of high pressures studied in this work.

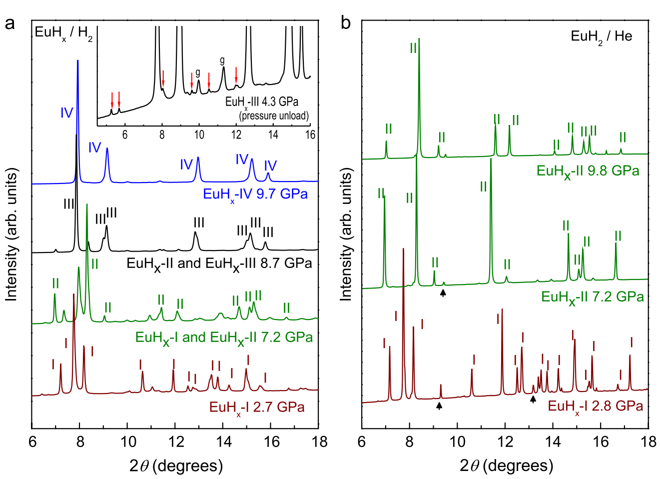

FIG. 1 (color online). Integrated XRD profiles of (a) the EuH_x/H_2 and (b) the EuH_2/He. The inset graph in (a) indicates the XRD profile of EuH_x -III at 4.3 GPa when pressure is unloaded. The downward arrows in the inset graph show the satellite peaks of the EuH_x-III phase. The "g" labels and upward arrows in (b) show the diffraction peaks of Re-metal gasket and EuO, respectively.

We performed a structure analysis by indexing, space-group determination, and Rietveld refinement. The diffraction peaks were indexed using the program X-CELL from Accelrys, Inc. [18]. The energy stability and H-atom positions in each phase were investigated using the density functional theory (DFT) program CASTEP [19]. We employed the generalized gradient approximation (GGA)-Perdew-Burke-Ernzerhof for solids (PBEsol) exchange-correlation functionals and used an ultrasoft pseudopotential [20,21]. The lattice parameters were set to the experimental values and the atomic positions were optimized to minimize the total energy.

For the EuH_x-II phase at 7.2 GPa, a good fit was obtained with a structure model of the space group of $P6_3/mmc$ [Z(Eu) = 2] with lattice parameters $a = 3.927$ Å and $c = 5.243$ Å, and a cell volume $V = 70.00$ Å^3. DFT calculations suggest a Ni_2In-type structure, where H atoms occupy special $2a$ and $2d$ positions, as the most probable structure model. The atomic positions were determined to be Eu:$2c(1/3, 2/3, 1/4)$, H1:$2a(0, 0, 0)$ and H2:$2d(2/3, 1/3, 1/4)$. The EuH_x-II can be considered to be divalent, as an cubic phase, which has been observed commonly for trivalent metal dihydrides, did not appear in EuH_2/He. The *Pnma* ($PbCl_2$ − type) → $P6_3/mmc$(Ni_2In − type) transition has been commonly reported for heavy alkaline-earth metal dihydrides and YbH_2 under high pressures [22–26], indicating this type of transition is possibly a characteristic of divalent metal dihydrides.

The analysis of EuH_x-III uses the single-phase XRD profile at 4.3 GPa [inset graph in Fig. 1(a)]. The EuH_x-III diffraction profile was indexed with 22 peaks, and a tetragonal lattice that formed a $\sqrt{5} \times \sqrt{5} \times 1$ superstructure of an original body-centered tetragonal (bct) lattice was found. The following 11 space-group numbers are allowed for the tetragonal cell by the extinction rule:140, 108, 120, 87, 121, 79, 82, 119, 139, 107, and 97. Among them, 87, 79, 82, 139, and 107 can realize the distorted bct lattice of EuH_x-III. A structure model with the space-group $I4/m$, $a = 8.351$ Å, $c = 5.352$ Å, $V = 373.19$ Å^3, and Z(Eu) = 10, shows an excellent fit to the diffraction profile at 4.3 GPa. The most probable structure model for EuH_x-III is shown in Fig. 2(a), together with the result of Rietveld fitting and atomic positions. The small spheres indicate the possible hydrogen positions. The diffraction profile of EuH_x-IV was indexed to a bct unit cell with lattice parameters $a = 3.654$ Å, and $c = 5.211$ Å, $V = 69.59$ Å^3, and Z(Eu) = 2 at 9.7 GPa. A structure model with the space-group $I4/mmm$ that contained two Eu atoms could fit the diffraction profile [Fig. 2(b)]. In our DFT calculation for EuH_x-III and IV, structure models with composition EuH_x ($x > 2$) were found to be more energetically favorable than with $x = 2$.

In order to investigate the hydrogen composition x in EuH_x-III and EuH_x-IV, we compared the atomic volume per Eu, i.e., $V_{\mathrm{atom,Eu}}$, at the transition pressures. $V_{\mathrm{atom,Eu}}$ is calculated from the refined unit cell parameters and plotted as a function of pressure in Fig. 3. We observe a volume expansion of 1.1 Å^3 in EuH_x/H_2 at 8.7 GPa, where EuH_x-II and EuH_x-III coexist. We make a rough estimate for it on the basis of the empirical observation that the absorption of a H atom into a rare-earth metal lattice induces 4 ± 0.5 Å^3 atomic volume expansion in the host metal lattice at ambient pressure. Under high pressure, the anticipated volume expansion should be less than that at ambient pressure. Assuming that the volume expansion results only from the absorption of hydrogen atoms, the increase Δx in the hydrogen composition in the II → III transition can be estimated as at least 0.2. The plots of EuH_x-III and EuH_x-IV in Fig. 3 lie on the same curve representing one equation of state. Thus, x differs very slightly between EuH_x-III and EuH_x-IV, which can now be represented as EuH_x ($x > 2$). In EuH_x-I and EuH_x-II, octahedral (O) sites have larger volume than tetrahedral (T) sites and are occupied by at least one H atom. On the assumption that H atoms occupy interstitial sites in same manner, each O site is thought to be fully occupied by at least a hydrogen atom and T sites are randomly occupied so that x exceeds 2.2 in EuH_x-III and EuH_x-IV.

We investigated the valence states of EuH_x/H_2 by synchrotron Mössbauer spectroscopy measurements. Figure 4 shows the typical Mössbauer spectra of EuH_x at 2.7 and 14.3 GPa. The velocity scale was calibrated relative to the single line of EuF_3 at ambient pressure. The spectra were fitted as a single peak. The isomer shift at 2.7 GPa, where the sample is in EuH_x-I phase, was -10.50 mm/s relative to the Eu^{3+}:EuF_3, indicating the divalent state. At 14.3 GPa, the isomer shift changed to 0.71 mm/s, showing that EuH_x-IV was in the trivalent state. This is clear evidence for the hydrogen-induced valence transition of EuH_x.

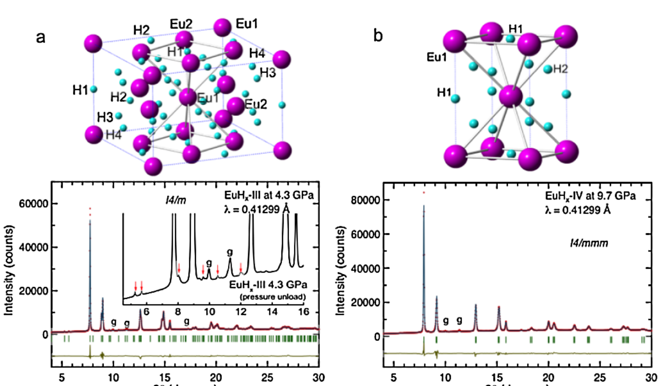

Elements	WyckLet.	x	y	z	Occ.
Eu1	2a	0	0	0	1
Eu2	8h	0.4129	0.2064	0	1
H1	2b	0	0	1/2	1
H2	8h	0.0914	0.3077	0	1
H3	16i	0.2022	0.1078	0.2396	r
H4	4d	0	1/2	1/4	r

Elements	WyckLet.	x	y	z	Occ.
Eu1	2a	0	0	0	1
H1	2b	0	0	1/2	1
H2	4d	0	1/2	1/4	r

FIG. 2 (color online). Structure models for (a) EuH_x-III and (b) EuH_x-IV, with corresponding Rietveld fits, the observed XRD profile and atomic positions. Large and small spheres indicate Eu-atoms and the possible H-atom positions, respectively. The final fit resulted in reliability factors of $R_{wp} = 4.32\%$, $R_p = 2.83\%$, and R_{wp}(without background) = 11.52%. The "r" in atomic position tables indicates that the T sites, H3 and H4 in EuH_x-III, H_2 in EuH_x-IV, are randomly occupied.

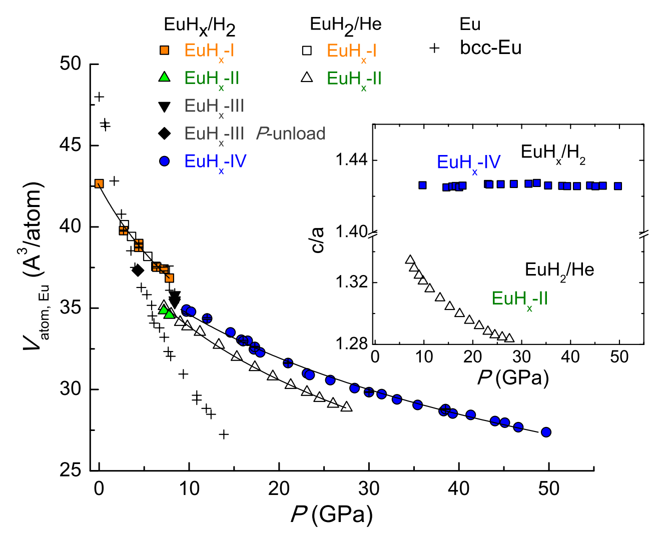

FIG. 3 (color online). Pressure dependence of $V_{\mathrm{atom,Eu}}$. The solid lines represent the Birch-Murnaghn equation of state (BM-EOS). The fitting to BM-EOS gives the following results: $B_0 = 10.17(3)$ GPa and $V_0 = 42.52(8)$ Å^3 for EuH_x -I, $B_0 = 11.2(2)$ GPa and $V_0 = 39.8(1)$ Å^3 for EuH_x -II, $B_0 = 14.33(7)$ GPa and $V_0 = 32.82(3)$ Å^3 for EuH_x -IV. The volume data of pure bcc-Eu were taken from Ref. [17]. The inset graph shows the pressure dependence of the $c/$textita ratio for EuH_x-II, EuH_x-III and EuH_x-IV. EuH_x-IV is stable up to the highest pressure of 50 GPa.

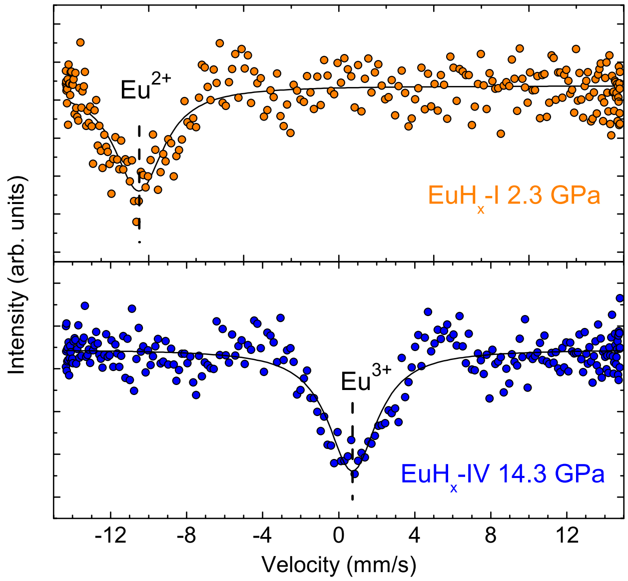

FIG. 4 (color online). High-pressure Eu-Mössbauer spectra of EuH_x-I at 2.3 GPa and EuH_x-IV at 14.3 GPa. The solid lines are fit of the experimental data. The velocity scale was calibrated relative to the center of a single line of EuF_3 under ambient conditions.

On the basis of Mössbauer measurement results, the EuH_x-IV may be thought as EuH_3, as the charge transfer from Eu to H is thought to drive the valence changes. Therefore, the hydrogen compositions of EuH_x-III and EuH_x-IV are considered to lie between 2.2 and 3.

We compare the EuH_x-IV phase with other rare-earth metal hydrides. The fcc structure is a bct structure whose c/a ratio is $\sqrt{2}$. EuH_x-IV with $c/a = 1.425$ is a slight (0.8%) distortion of fcc. Because of its trivalent character and the small distortion from the fcc structure, EuH_x-IV corresponds to the β phase observed commonly for other rare-earth metal hydrides.

In summary, we offer the following conclusions. The external pressure, by a thermodynamic effect, drives the $EuH_x - \mathrm{I}(x = 2, Pnma) \rightarrow \mathrm{II}(x = 2, P6_3/mmc)$ transition at 7.2 GPa. EuH_x-I and EuH_x-II are in the divalent state. At around 8.7 GPa, the EuH_x-II phase reacts with the surrounding high-pressure hydrogen. The penetration of H atoms induces the $Eu^{2+} \rightarrow Eu^{3+}$ valence change and the formation of EuH_x-III ($x > 2$, $I4/m$) and IV ($x > 2$, $I4/mmm$) phases. With the small distortion from the fcc structure and its trivalent character, EuH_x-IV can be categorized as a β phase, which has been observed for other rare-earth metal hydrides. This is the first observation of a β phase and the trivalent state for EuH_x. Henceforth, EuH_x is no longer an irregular member of the rare-earth metal hydrides.

This work was supported by the New Energy Development Organization (NEDO) under Advanced Fundamental Research on Hydrogen Storage Materials. Thanks are due to J. S. Schilling of Washington University in St.Louis, and R. W. McCallum and K. W. Dennis of the Materials Preparation Center, Ames Laboratory, for providing the high-purity Eu sample. XRD and Mössbauer experiments were performed at BL10XU (Proposal numbers 2009B1010 and 2010A1004) and BL09XU in SPring-8 (Proposal number 2010B1244), respectively.

*matsuoka@cqst.osaka-u.ac.jp

[1] P. Vajda, in *Handbook on the Physics and Chemistry of Rare Earths*, edited by K. A. Gschneidner and L. Eyring (Elsevier Science B. V., Amsterdam, 1995), Vol. 20, p. 207.
[2] M. Tkacz and T. Palasyuk, J. Alloys Compd. **446–447**, 593 (2007).
[3] S. M. Filipek, J. Adv. Science **19**, 1 (2007).
[4] A. Machida, A. Ohmura, T. Watanuki, K. Aoki, and K. Takemura, Phys. Rev. B **76**, 052101 (2007).
[5] A. Ohmura, A. Machida, T. Watanuki, K. Aoki, S. Nakano, and K. Takemura, J. Alloys Compd. **446–447**, 598 (2007).
[6] J. S. Olsen, J. E. Jorgensen, and L. Gerward, Hasy Lab Annual Report, 2003.
[7] K. Hardcastle and J. Warf, Inorg. Chem. **5**, 1728 (1966).
[8] W. Iwasieczko, M. Drulis, and H. Drulis, J. Alloys Compd. **327**, 11 (2001).
[9] K. Hirano, J. Kadono, S. Yamamoto, T. Tanabe, and H. Miyake, J. Alloys Compd. **408–412**, 351 (2006).
[10] H. Sugimoto and Y. Fukai, Acta Metall. **40**, 2327 (1992).
[11] H. K. Mao, J. Xu, and P. M. Bell, J. Geophys. Res. **91**, 4673 (1986).
[12] Y. Ohishi, N. Hirao, N. Sata, K. Hirose, and M. Takata, High Press. Res. **28**, 163 (2008).
[13] H. Fujihisa (unpublished).
[14] M. Seto, R. Masuda, S. Higashitaniguchi, S. Kitao, Y. Kobayashi, C. Inaba, T. Mitsui, and Y. Yoda, Phys. Rev. Lett. **102**, 217602 (2009).
[15] W. Bi, Y. Meng, R. S. Kumar, A. L. Cornelius, W. W. Tipton, R. G. Hennig, Y. Zhang, C. Chen, and J. S. Schilling, Phys. Rev. B **83**, 104106 (2011).
[16] W. A. Grosshans and W. B. Holzapfel, Phys. Rev. B **45**, 5171 (1992).
[17] K. Takemura and K. Syassen, J. Phys. F **15**, 543 (1985).
[18] M. A. Neumann, J. Appl. Crystallogr. **36**, 356 (2003).
[19] S. J. Clark, M. D. Segall, C. J. Pickard, P. J. Hasnip, M. I. J. Probert, K. Refson, and M. C. Payne, Z. Kristallogr. **220**, 567 (2005).
[20] J. P. Perdew, A. Ruzsinszky, G. I. Csonka, O. A. Vydrov, G. E. Scuseria, L. A. Constantin, X. Zhou, and K. Burke, Phys. Rev. Lett. **100**, 136406 (2008).
[21] D. Vanderbilt, Phys. Rev. B **41**, 7892 (1990).
[22] J. S. Olsen, B. Buras, L. Gerward, B. Johansson, B. Lebech, H. L. Skriver, and S. Steenstrup, Phys. Scr. **29**, 503 (1984).
[23] K. Kinoshita, M. Nishimura, Y. Akahama, and H. Kawamura, Solid State Commun. **141**, 69 (2007).
[24] J. S. Smith, S. Desgreniers, J. S. Tse, and D. D. Klug, J. Appl. Phys. **102**, 043520 (2007).
[25] J. S. Tse, D. D. Klug, S. Desgreniers, J. S. Smith, R. Flacau, Z. Liu, J. Hu, N. Chen, and D. T. Jiang, Phys. Rev. B **75**, 134108 (2007).
[26] J. S. Smith, S. Desgreniers, D. D. Klug, and J. S. Tse, Solid State Commun. **149**, 830 (2009).